

The function of phosphatidylinositol 5-phosphate 4-kinase γ (PI5P4K γ) explored using a specific inhibitor that targets the PI5P binding site.

Jonathan H. Clarke* \dagger , Maria-Luisa Giudici* \dagger , John E. Burke \ddagger \S , Roger L. Williams \ddagger ,
David J. Maloney \P Juan Marugan \P & Robin F. Irvine*

* Department of Pharmacology, Tennis Court Road, Cambridge CB2 1PD, UK

\ddagger MRC Laboratory of Molecular Biology, Francis Crick Avenue, Cambridge CB2 0QH, UK

\P National Center for Advancing Translational Sciences, 9800 Medical Center Drive, Rockville, MD 20850, USA

\S Present address: Department of Biochemistry and Microbiology, University of Victoria, 270a Petch Hall, Victoria, BC, Canada

\dagger These authors contributed equally to this study.

Page heading title: Phosphatidylinositol 5-phosphate 4-kinase γ inhibition

Corresponding author, R.F. Irvine rfi20@cam.ac.uk Phone 44-1223-334177 FAX 44-1223 334040

Keywords: Phosphatidylinositol 5-phosphate; phosphatidylinositol 5-phosphate 4-kinase γ ; PI5P; PI5P4K; PI5P4K γ

Abbreviations: PI5P, phosphatidylinositol 5-phosphate; PI(4,5)P₂, phosphatidylinositol 4,5,-bisphosphate; HDX-MS, Hydrogen-deuterium exchange mass spectrometry.

Abstract

NIH-12848 (NCGC00012848-02), a putative phosphatidylinositol-5-phosphate 4-kinase γ (PI5P4K γ) inhibitor, was explored as a tool for investigating this enigmatic, low activity, lipid kinase. PI5P 4-kinase assays *in vitro* showed that NIH-12848 inhibited PI5P4K γ with an IC₅₀ of approximately 1 μ M but did not inhibit the α and β PI5P4K isoforms at concentrations up to 100 μ M. A lack of inhibition of PI5P4K γ ATPase activity suggested that NIH-12848 does not interact with the enzyme's ATP binding site, and direct exploration of binding using hydrogen-deuterium exchange mass spectrometry revealed the putative PI5P-binding site of PI5P4K γ to be the likely region of interaction. This was confirmed by a series of mutation experiments, which led to the identification of a single PI5P4K γ amino acid residue that can be mutated to its PI5P4Ks α and β homologue to render PI5P4K γ resistant to NIH-12848 inhibition. 10 μ M NIH-12848 was applied to cultured mouse principal kidney cortical collecting duct (mpkCCD) cells, which we show express PI5P4K γ that increases when the cells grow to confluence and polarise. NIH-12848 inhibited the translocation of Na⁺/K⁺ATPase to the plasma membrane that occurs when mpkCCD cells grow to confluence, and also prevented reversibly their forming of 'domes' on the culture dish. Both these NIH-12848-induced effects were mimicked by specific RNAi knock-down of PI5P4K γ , but not that of PI5P4Ks α or β . Overall the data reveal a likely contribution of PI5P4K γ to the development and maintenance of epithelial cell functional polarity, and show that NIH-12848 is a potentially powerful tool for exploring the cell physiology of PI5P4Ks.

Introduction

The phosphatidylinositol 5-phosphate 4-kinases (PI5P4Ks) are a family consisting of three isoforms in mammals (α , β , and γ), whose most likely function is currently believed to be the regulation of the levels of their substrate, PI5P (see refs [1, 2] for reviews). While the α and β isoforms have had some physiological and pathological functions assigned to them, including in gene regulation [3, 4], stress responses [5], insulin signalling [6] and cancer [7, 8], PI5P4K γ is hardly understood at all. It is apparently ubiquitously expressed, but at very different levels between tissues, being particularly high in epithelial cells of the thick ascending limb of the kidney and collecting ducts cells [9] and in specific neurons in brain [10]. It apparently has a vesicular localization [9, 10], may have a functional connection with Rho [11], shows a much lower enzymatic activity *in vitro* than the other PI5P4K isoforms [12], and can heterodimerise *in vitro* with PI5P4K α [12] (note that extensive heterodimerisation between PI5P4Ks α and β has been shown to occur *in vivo* [13, 14]).

Specific inhibitors of enzymes can be useful tools in studying their function, and kinase inhibitors are among those that have shown most promise as potential therapeutic agents. Recently the characterization of inhibitors for PI5P4K α [15] and PI5P4K β [16] have raised that hope for those isoforms, but the isoform specificity of neither inhibitor has yet been established, and so far no such tools exist at all for PI5P4K γ . Moreover, a challenge facing any kinase inhibitor, the great majority of which interact with the ATP-binding site of their target, is for it to have both sufficient specificity (because all kinase ATP binding sites show some structural similarity) and potency (cellular concentrations of ATP are in the millimolar range, so nanomolar affinity of an inhibitor is often required for micromolar efficacy in a cell). The high affinity and specificity of the PI 3-kinase δ inhibitor PIK-39 that results from a remarkable induced fit into the ATP binding site of its target protein [17] is one example of an ATP binding site competitor that overcomes these issues. A potential approach for increasing the kinase specificity is to look for ATP-allosteric modulators, although in some cases (e.g. [18]) there are discrepancies between cell-based and isolated kinase inhibitory assays, making difficult the finding of this kind of inhibitor.

Herein we report the characterization and use of a PI5P4K γ -specific inhibitor NIH-12848 (full designation NCGC00012848-02), which we show interacts not with the ATP binding site but with the region where PI5P probably binds, including the activation loop. We use the inhibitor to begin the first exploration, in a kidney epithelial cell line, of the function of PI5P4K γ . Also, we show how we can mutate PI5P4K γ so that it becomes insensitive to NIH-12848, opening the possibility of chemical biology to explore the functions of all three PI5P4Ks.

Materials and Methods

Enzyme preparation and mutagenesis

Recombinant enzyme was prepared essentially as described previously [12]. Protein from *PIP4K2C* (UniGene 6280511) or associated mutants, cloned into the expression vector pGEX6P (GE Healthcare) was expressed and purified from *E. coli*

BL21(DE3). Cultures were induced with 0.4 mM IPTG and probe-sonicated in the presence of protease inhibitors. GST fusion proteins of PI5P4K γ and PI5P4K γ +, a mutant with specific activity close to that of the active PI5P4K α isoform [12], were harvested by binding to glutathione sepharose beads (GE Healthcare) and cleaved *in situ* with 50U of PreScission protease (GE Healthcare) for 4 hours at 4°C. Purity was confirmed by SDS-PAGE and protein concentration determined by colorimetric assay (Bio-Rad). Site-directed mutagenesis using the QuikChange technique (Agilent Technologies) was used to generate clones from which mutant forms of PI5P4K γ and PI5P4K γ + were produced (for mutagenesis primers see Table S1).

Biochemical assays

Lipid kinase assays were performed as described previously [13]. DiC16-PI5P was purchased from Echelon Biosciences, and after drying down in Eppendorf tubes was sonicated for 3 x 30 seconds in a Decon Ultrasonics sonicating bath. This lipid substrate (6 μ M PI5P) and recombinant lipid kinase were added to the reaction mixture (200 μ l final volume) with 10 μ Ci [γ -³²P]ATP and incubated at 30°C for 10-60 min. Lipids were extracted using an acidic phase-separation [19] and separated by one-dimensional thin layer chromatography (2.8:4:1:0.6 chloroform:methanol:water:ammonia). Radiolabelled PI(4,5)P₂ spots were detected by autoradiography, extracted and counted with Ultima Gold XR scintillant (Packard) on a LS6500 scintillation counter (Beckman Coulter). Intrinsic ATPase activities of the enzymes were determined using the Transcreener ADP² fluorescence polarization method (BellBrook Labs). A range of enzyme concentrations was assayed with ATP substrate (100 μ M ATP, 60 min incubation at 22°C) and polarization units (mP) were read using a PHERAstar Plus microplate reader (BMG Labtech). Experimental values were interpolated from an ADP/ATP utilization standard curve and plotted using nonlinear regression analysis with Prism 5.

Hydrogen Deuterium Exchange Mass Spectrometry

Hydrogen deuterium exchange mass spectrometry experiments were performed according to previously published protocols [20, 21]. In brief, HDX reactions were initiated in HDX buffer (20 mM HEPES pH 7.5, 50 mM NaCl, 2 mM Tris Carboxyl Ethyl Phosphine (TCEP)) by the addition of 98% D₂O Solution (10 mM HEPES pH 7.5, 50 mM NaCl, 2 mM TCEP), to give a final concentration of 78% D₂O. Final protein concentrations were 1 μ M. For all reactions with inhibitor there was a ten fold excess of inhibitor to protein, and this was allowed to incubate for 30 minutes on ice before initiation of H/D exchange. Four time points of exchange were carried out (3 s, 30 s, and 300 s at 23 °C and 3 s at 0 °C), and were terminated by the addition of a quench buffer (1 M guanidine-HCl, 0.8% formic acid), followed by snap freezing in liquid nitrogen. Samples were stored at -80 °C until mass analysis.

Measurement of Deuterium Incorporation

Protein samples were rapidly thawed and injected onto a UPLC column immersed in ice as previously described [21]. The protein was run over two immobilized pepsin columns in series (Applied Biosystems; porosyme, 2-3131-00) at 200 μ L/min for 3 min and collected over a van-guard pre-column trap (Waters). The trap was subsequently eluted in line with an Acquity 1.7 μ m particle, 100 mm x 1 mm C18 UPLC column (Waters), using a gradient of 5-36% B (buffer A 0.1% formic acid, buffer B 100% acetonitrile) over 20 min. Eluent from the column was injected

onto a Xevo QTOF (Waters) acquiring over a mass range from 350 to 1500 m/z , with an electrospray ionization (ESI) source operated at a temperature of 225 °C, and a spray voltage of 2.5 kV.

Protein Digestion, Peptide Identification, and Mass Analysis

Peptide identification was done by running tandem MS/MS experiments using a 3-35% B gradient over 120 min with a Xevo QTOF (Waters). This was supplemented with a 20 min gradient separation to identify and correct the retention time for all samples. The MS tolerance was set to 3 ppm with an MS/MS tolerance at 0.1 Da. The resulting MS/MS datasets were analyzed with the Mascot search within Mascot distiller (matrix science). All peptides with a Mascot score >15 were analyzed using HD-Examiner Software (Sierra Analytics). The full list of peptides was then manually validated by searching a non-deuterated protein sample's MS scan to test for the correct m/z state, and check for the presence of overlapping peptides. Ambiguously identified peptides were excluded from all subsequent analysis. The first round of analysis and identification were performed automatically by the HD-Examiner software, but all peptides (deuterated and non-deuterated) were manually verified at every state and time point for the correct charge state, m/z range, presence of overlapping peptides, and the expected retention time. All HDX-MS results are presented as relative levels of deuterium incorporation, and no correction for back exchange is applied, because no fully deuterated protein sample could be obtained.

Cell Culture

Immortalized mouse cortical collecting duct (mpkCCD) cells [22, 23] were grown in defined medium (DMEM:Ham's F12 1:1 vol/vol, 60 nM sodium selenate, 5 $\mu\text{g/ml}$ transferrin, 2 mM glutamine, 50 nM dexamethasone, 1 nM triiodothyronine, 10 ng/ml epidermal growth factor, 5 $\mu\text{g/ml}$ insulin, 20 mM D-glucose, 2% vol/vol fetal calf serum, and 20 mM HEPES, pH 7.4) at 37°C in a 5% CO₂-95% air atmosphere. Medium was changed every two days and all studies were performed on cells that had been grown on plastic Petri dishes or glass slides.

RNAi

Depletion of specific PI5P4K isoforms was achieved by transfecting cells with small interference RNAs (siRNAs) specific to each PI5P4K isoform. The siRNAs were obtained from Thermo Scientific Dharmacon (ON-TARGET^{plus} SMART pool). Control siRNAs were sequences that would not be recognised by any part of the mouse genome. MpkCCD cells were plated at a density of 6×10^4 per well (24 well/plate) one day before transfection, then were transfected with each siRNA at a final concentration of 25 pmol/ml using DharmaFECT 1 Transfection Reagent (Dharmacon). At 72-h post-transfection, a new round of transfection was performed, and the cells were cultured for another 48 h.

Morphological and immunocytochemical studies

Confluent cells grown on plastic Petri dishes were examined under an inverted microscope (Zeiss) equipped with phase-contrast optics. Indirect immunofluorescence studies were performed on confluent cells grown on glass slides fixed with ice-cold methanol or 4% formaldehyde. Cells were processed for immunofluorescence using anti-Na⁺/K⁺-ATPase α -1 monoclonal antibody (Millipore) and anti-ZO-1 polyclonal antibodies (Millipore), and were examined under a Leica confocal microscope.

Western Blotting

Cells were grown to confluence, washed in cold PBS, and lysed by scraping them off in boiling Laemlli sample buffer containing 20mM β -mercaptoethanol. Lysate was boiled for 5 min, and viscosity was reduced by sonication using four bursts of 30 sec each with 15 sec on ice between each sonication step. Lysate was boiled as before and centrifuged at 20000xg for 5 min. The supernatant was run on 10% poly-acrylamide gels, transferred to nitrocellulose membranes, blocked in TBS-0.05% Tween 20/5% non-fat dry milk and probed with antibodies diluted in the same solution. The following primary antibodies were used: polyclonal anti-PI5P4K γ 1:2500 [9], monoclonal anti- α tubulin 1:5000 (SIGMA). After washing in TBS-0.05% Tween and incubation with secondary antibody, protein was detected by Super Signal West Femto Maximum Sensitivity Substrate (Thermo Scientific).

QT-PCR

Cellular RNA was extracted with Trizol reagent (Invitrogen) and 1 ng was reverse transcribed with Superscript III and random hexamers (Invitrogen). Quantification of gene expression of the three PI5P4K isoforms was assessed by using TaqMan Gene Expression Assays and TaqMan Gene Expression Master Mix (Life Technologies), using TATA-box binding protein (TBP) as the reference gene.

Results and Discussion

NIH-12848 is a specific PI5P4K γ inhibitor

NIH-12848 (Fig 1) initially emerged as ‘compound 1’ from a kinome profiling study, measuring its selectivity against a panel of 460 kinases (see ref [24] Supplementary Figure 3). As can be seen in the supporting information (Supplementary Table S2), NIH-12848 was exquisitely selective for PI5P4K γ , with an apparent IC₅₀ of 2-3 μ M (Fig S1). This screen did not include PI5P4K α (Fig S2), and to clarify the actions of NIH-12848 against PI5P4Ks we tested it in PI5P 4-kinase assays using PI5P and ³²P- γ -ATP as substrates (see Methods). Under these conditions, PI5P4K α was not inhibited by 100 μ M NIH-12848 (Fig S3A), and PI5P4K β showed a small but significant stimulation at the same concentration (Fig S3B), whereas PI5P4K γ was inhibited with an apparent IC₅₀ of 3.3 μ M (Fig 2), similar to the apparent K_d in the kinome profiling (above).

Because PI5P4K γ has a very low catalytic activity [12] these assays use a final enzyme concentration of around 2.3 μ M, so it is possible that NIH-12848 is actually more potent and we are in part titrating the enzyme protein. We therefore also tested NIH-12848 on nanomolar levels of the PI5P4K γ + mutant [12], which has a 300-fold higher activity than wild type PI5P4K γ , and we found the IC₅₀ of NIH-12848 to be about 1 μ M (Supp Fig 3C). Below we show that the PI5P binding site is the likely site of interaction for NIH-12848, and because the lipid PI5P does not have a precise concentration (not least this depends on its physicochemical structure), the number we deduce here can only be an empirical IC₅₀, not an absolute K_i.

NIH-12848 interacts with the PI5P binding site on PI5P4K γ

Most of the mutations introduced into PI5P4K γ to create PI5P4K γ + [12] involve the changing of residues that bind or stabilise ATP to the equivalent residues present in the much more active PI5P4K α . So the marked contrast in sensitivities to NIH-12848 of PI5P4K γ + versus PI5P4K α suggested that NIH-12848 could be

unusual among kinase inhibitors in that it might not be interacting with the ATP binding site. This possibility was supported by an inability of NIH-12848 to inhibit the intrinsic ATPase activity of PI5P4K γ (Fig 2B), and by the observation that including 100 μ M ATP in assays using PI5P4K γ^+ (K_m for ATP, 2 μ M [12]) had only a small effect on the ability of NIH-12848 to inhibit the enzyme near its IC_{50} concentration: 2 μ M NIH-12848 inhibited PI5P4K γ^+ by 40 \pm 3.2% with carrier-free (approx. 16 nM) ATP, and 64 \pm 2.8% with 100 μ M ATP; the small shift in NIH-12848 sensitivity is probably an allosteric effect (see below).

To determine directly the interaction site of NIH-12848 with PI5P4K γ and PI5P4K γ^+ we turned to hydrogen deuterium exchange mass spectrometry (HDX-MS), a powerful tool for mapping protein conformational changes, and binding epitope sites of interaction on proteins [21, 25]. There are two peptides in PI5P4K γ whose rate of HDX is altered significantly in the presence of NIH-12848 (Fig 3B-D). One peptide spans residues 373-407 (Fig 3C,D), part of the enzyme's activation loop, which has been shown to govern the substrate specificity of PI5P4Ks and PI4P5Ks [26, 27]. There was also a change in a peptide spanning residues 158-162 (Fig 3C,D), which is part of an α -helix that is near the activation loop in PI5P4K γ [28], designated α -helix 4 in the original annotated PI5P4K β structure ([29]), see Fig 3B,F). Intriguingly, in the PI5P4K γ^+ there was a significant increase in exchange in residues 158-162 compared to wild-type PI5P4K γ , and a correspondingly larger decrease in exchange upon addition of NIH-12848 (Fig 3E). These data point to the proposed PI5P-binding site of PI5P4Ks [26, 27, 29] as the likely area of NIH-12848 interaction.

PI5P4K γ can be made resistant to NIH-12848

Direct competition experiments (increasing PI5P and looking at the effect that this has on NIH-12848 potency *in vitro*) would be the most direct route to confirming the above suggestion. However, NIH-12848 is a hydrophobic compound, as is PI5P, and it is likely that the two compounds would form mixed micellar structures when together in aqueous buffers, so any such 'competition' would be uninterpretable. To seek confirmation for the site of interaction of NIH-12848 we therefore undertook a series of mutational experiments, focusing on the regions of interaction suggested by the HDX-MS data. In the region 373-407 (see above), only glutamine 378 differs between PI4P5K isoforms and mutating this residue to the PI5P4K α equivalent histidine made no detectable difference to the activity or NIH-12848 sensitivity of the enzyme (data not shown). In residues 158-162 (see above), isoleucine 159 and aspartate 161 are both valines in PI5P4Ks α and β , and mutating these together in PI5P4K γ^+ caused a small shift in sensitivity to NIH-12848 (inhibition by 10 μ M NIH-12848 was 96% \pm 1.5 in WT PI5P4K γ^+ and 71% \pm 2.6 in the (E378H,I159V,D161V) PI5P4K γ^+ mutant).

Examining this region closely in the structure (Fig 3F) suggested three other residues that might interact with the substrate or inhibitor and which are different between PI5P4Ks γ versus α/β . These are serine 164, asparagine 165, and glutamate 153, which are respectively asparagine, isoleucine and threonine in PI5P4K α/β ; of these, glutamate 153 has already been mutated to the PI5P4K α/β -equivalent threonine in creating PI5P4K γ^+ [12]. We therefore introduced all five mutations of potential interest (Q378H, I159V, D161V, S164N, N165I) into PI5P4K γ and PI5P4K γ^+ , and both these mutant enzymes were completely resistant to NIH-12848 inhibition (Fig S4A,B).

These data support the HDXMS data suggesting that NIH-12848 is binding to this area of the PI5P4K γ protein, and they also imply that serine 164 and/or

asparagine 165 are the major contributors to the sensitivity of PI5P4K γ to NIH-12848. So we mutated only those two residues in PI5P4K γ to their PI5P4Ks α/β homologues individually or together, and found that while S164N PI5P4K γ is as sensitive to NIH-12848 inhibition as wild type PI5P4K γ (Fig S4C), N165I PI5P4K γ is completely insensitive, with 50 μ M NIH-12848 having no effect on this mutant (Fig 4). Note that the activity of N165I PI5P4K γ was 6.7x higher than wild type PI5P4K γ in these assays, and Fig S4D summarises the activities and sensitivities to NIH12848 of the mutants discussed here.

Overall these data show that asparagine 165 is the residue in PI5P4K γ that is almost entirely responsible for its sensitivity to NIH-12848. There was no detectable change in the amide exchange rate at N165 when NIH-12848 binds to PI5P4K γ or PI5P4K γ + (Fig 3), and the simplest interpretation is that NIH-12848 binds to the activation loop and α -helix 4 to induce a change in the structure in this region, and that introducing an isoleucine (as in PI5P4Ks α and β) at residue 165 prevents this structural change from happening, perhaps because of a hydrophobic interaction with the activation loop (see Fig 3F). Whatever the molecular mechanism, this residue could in the future be mutated in both alleles of the PI5P4K γ gene in a cell line or a mouse to engender NIH-12848 resistance of the PI5P4K γ , which would be a powerful chemical biology approach to eliminate completely any potential non-specific cellular effects of NIH-12848. Introducing the complementary mutations into PI5P4Ks α or β , possibly to make them NIH-12848-sensitive, could be an equally informative avenue of investigation.

Effects of NIH-12848 on a kidney cell line

PI5P4K γ is widely expressed in mammalian tissues, but is particularly high, and is indeed the principal PI5P4K isoform, in kidney [9]. It is expressed there in epithelial cells, particularly in the thick ascending limb and cortical collecting duct, so to explore its cellular functions we chose mpkCCD cells, a cell line derived from epithelial cells in the cortical collecting duct of the kidney [22, 23]. Western blotting confirmed an easily detectable level of expression of PI5P4K γ in mpkCCD cells (Fig 6A). These cells grow to confluence and then form gap junctions between them. They then begin to form ‘domes’ in which process, they show a property of transporting epithelia when cultured *in vitro* on solid supports. ‘Domes’ are fluid-filled blisters formed between the solid growth surface and the cell layer, and their formation is regarded as a sign of differentiated epithelia with active transport processes and with an intact epithelial barrier due to functional cell-cell contacts [22, 23]. We found using quantitative PCR that while reaching confluence there is a 3-fold increase in PI5P4K γ mRNA, but no significant change in the two other PI5P4K isoforms (Table 1). We thought that PI5P4K γ might be involved in epithelial cell polarity because in adult mammalian kidney PI5P4K γ is present in intracellular vesicles with a distribution polarised towards the lumen [9], and in zebra fish (*Danio*) it is highly expressed in the pro-nephric duct throughout development (ZFIN Database: ZDB-IMAGE-030829-506).

One easily monitored parameter is the redistribution of Na⁺/K⁺ ATPase from the cytoplasm to the basolateral plasma membrane that occurs when the cells reach confluence [30]. We explored the effect of 10 μ M NIH-12848 (1 μ M had similar but smaller effects) and found a complete inhibition of this redistribution, while the cells remained healthy and confluent, with gap junctions formed as revealed by immunocytochemistry of ZO-1 (Fig 5A). From this, we suggest PI5P4K γ is involved in the progress towards a polarised epithelial phenotype.

Consistent with this possibility, the formation of ‘domes’ (see above) was also markedly inhibited (Fig 5B) by NIH-12848. Moreover, if NIH-12848 was added subsequent to dome formation, the domes disappeared with a detectable effect within 3 hours that was maximal by 24 hours (Fig 5B), indicating a dynamic relationship between PI5P4K γ and the development and maintenance of this morphology. The molecular mechanisms underlying this relationship will require much further investigation, but the reported link between PI5P4K γ and Rho [11], taken together with the well-known involvement of Rho in epithelial cell transport and polarity [31, 32], offers one possibility for exploration.

RNAi knock-down of PI5P4K γ

Our extensive molecular exploration of the interaction of NIH-12848 with PI5P4K γ (above) emphasizes its remarkable specificity, but nevertheless it is possible that the effects we see are due to an off-target action. To gather some independent evidence that inhibition of PI5P4K γ underlies the effects of NIH-12848, and thus to begin a validation of this inhibitor as a tool for exploring PI5P4K γ function, we knocked down PI5P4K γ in the mpkCCD cells by RNAi. Fig 6A and Table S3 shows that the knock-down was specific and successful, and Figs 6 B-C show the effects of PI5P4K γ knock-down on Na⁺/K⁺ATPase re-localisation (Fig 6B) and dome formation (Fig 6C). Within the limits of these analyses, both effects of NIH-12848 are mimicked by this knock-down.

Control experiments knocking down PI5P4K α and β did not show the same effect on dome formation. PI5P4K β knock-down had no detectable effect (Fig S5B), while knockdown of PI5P4K α had a pronounced opposite (stimulatory) effect (Fig S5A,B). We have no immediate explanation for this latter action, which we believe is likely to be independent of PI5P4K γ activity because knock-down of PI5P4K γ and PI5P4K α together showed that PI5P4K γ causes a similar and internally consistent inhibitory effect on the higher level of dome formation resulting from PI5P4K α knock-down (Fig S5C). Further studies, including using PI5P4K α inhibitors (e.g. ref [15]) will be required to clarify this function of PI5P4K α and its relationship with PI5P4K γ . We have discussed elsewhere [12] the possibility that PI5P4K γ may sometimes serve to target the more active PI5P4K α to a specific cellular location.

Overall these experiments yield the first functional insight into PI5P4K γ 's physiological role in epithelial cells. Much remains to be explored to clarify exactly what the enzyme is doing in this context, but the very similar effects induced in mpkCCD cells by inhibition with NIH-12848 and knock-down of PI5P4K γ are a crucial first stage in a proof of principle of the potential usefulness of NIH-12848 in such an exploration. Our detailed mapping and manipulation of the molecular interaction of NIH-12848 with PI5P4K γ also suggests ways to a wider use of this inhibitor in the exploration of functions of the PI5P4K family.

Acknowledgements

We are very grateful to Dr A. Vandewalle (INSERM U773, Paris, France) for provision of the mpkCCD cell line and Simon Bulley for his help and advice with the QT-PCR. J.H.C was supported by the MRC (Grant RG64071), M-L.G. by the BBSRC (Grant RG65394), and J.H.B. by the BHF (Grant PG11/109/29247).

Author contributions:

Jon Clarke engineered and produced recombinant proteins, performed *in vitro* assays and processed data; Maria-Luisa Giudici performed cell biology experiments and QT-PCR and processed data; John Burke performed the HDX-MS, processed data and interpreted protein structures; Roger Williams processed HDX-MS data and interpreted protein structures; David Maloney and Juan Marugan performed the initial discovery of the PI5P4K γ -NIH-12848 interaction; Robin Irvine performed some *in vitro* assays and processed data. All the authors discussed the results, interpreted data and co-wrote the paper.

References

- 1 Clarke, J. H., Wang, M. and Irvine, R. F. (2010) Phosphatidylinositol 5-phosphate 4-kinases: Localization, regulation and function of Type II phosphatidylinositol 5-phosphate 4-kinases. *Adv. Enz. Reg.* **50**, 12-18
- 2 Clarke, J. H. and Irvine, R. F. (2012) The activity, evolution and association of phosphatidylinositol 5-phosphate 4-kinases. *Adv. Biol. Reg.* **52**, 40-45
- 3 Shah, Z. H., Jones, D. R., Sommer, L., Foulger, R., Bultsma, Y., D'Santos, C. and Divecha, N. (2013) Nuclear phosphoinositides and their impact on nuclear functions. *The FEBS journal.* **280**, 6295-6310
- 4 Gelato, K. A., Tauber, M., Ong, M. S., Winter, S., Hiragami-Hamada, K., Sindlinger, J., Lemak, A., Bultsma, Y., Houliston, S., Schwarzer, D., Divecha, N., Arrowsmith, C. H. and Fischle, W. (2014) Accessibility of Different Histone H3-Binding Domains of UHRF1 Is Allosterically Regulated by Phosphatidylinositol 5-Phosphate. *Mol Cell.* **54**, 905-919
- 5 Keune, W. J., Jones, D. R. and Divecha, N. (2013) PtdIns5P and Pin1 in oxidative stress signaling. *Adv. Enz. Reg.* **53**, 179-189
- 6 Lamia, K. A., Peroni, O. D., Kim, Y. B., Rameh, L. E., Kahn, B. B. and Cantley, L. C. (2004) Increased insulin sensitivity and reduced adiposity in phosphatidylinositol 5-phosphate 4-kinase beta^{-/-} mice. *Mol. Cell. Biol.* **24**, 5080-5087
- 7 Emerling, B. M., Hurov, J. B., Poulgiannis, G., Tsukazawa, K. S., Choo-Wing, R., Wulf, G. M., Bell, E. L., Shim, H. S., Lamia, K. A., Rameh, L. E., Bellinger, G., Sasaki, A. T., Asara, J. M., Yuan, X., Bullock, A., Denicola, G. M., Song, J., Brown, V., Signoretti, S. and Cantley, L. C. (2013) Depletion of a putatively druggable class of phosphatidylinositol kinases inhibits growth of p53-null tumors. *Cell.* **155**, 844-857
- 8 Jude, J. G., Spencer, G. J., Huang, X., Somerville, T. D., Jones, D. R., Divecha, N. and Somerville, T. C. (2014) A targeted knockdown screen of genes coding for phosphoinositide modulators identifies PIP4K2A as required for acute myeloid leukemia cell proliferation and survival. *Oncogene.* 10.1038/onc.2014.77
- 9 Clarke, J. H., Emson, P. C. and Irvine, R. F. (2008) Localization of phosphatidylinositol phosphate kinase II γ in kidney to a membrane trafficking compartment within specialized cells of the nephron. *Am. J. Physiol. Renal Physiol.* **295**, F1422-1430
- 10 Clarke, J. H., Emson, P. C. and Irvine, R. F. (2009) Distribution and neuronal expression of phosphatidylinositol phosphate kinase II γ in the mouse brain. *J. Comp. Neurol.* **517**, 296-312

- 11 Yih, L. H., Wu, Y. C., Hsu, N. C. and Kuo, H. H. (2012) Arsenic trioxide induces abnormal mitotic spindles through a PIP4KIIgamma/Rho pathway. *Toxicological Sci.* **128**, 115-125
- 12 Clarke, J. H. and Irvine, R. F. (2013) Evolutionarily conserved structural changes in phosphatidylinositol 5-phosphate 4-kinase (PI5P4K) isoforms are responsible for differences in enzyme activity and localization. *Biochem. J.* **454**, 49-57
- 13 Wang, M., Bond, N. J., Letcher, A. J., Richardson, J. P., Lilley, K. S., Irvine, R. F. and Clarke, J. H. (2010) Genomic tagging reveals a random association of endogenous PtdIns5P 4-kinases II α and II β and a partial nuclear localisation of the II α isoform. *Biochem. J.* **430**, 215-221
- 14 Bultsma, Y., Keune, W. J. and Divecha, N. (2010) PIP4K β interacts with and modulates nuclear localisation of the high activity PtdIns5P-4-kinase isoform, PIP4K α . *Biochem. J.* **430**, 223-235
- 15 Davis, M. I., Sasaki, A. T., Shen, M., Emerling, B. M., Thorne, N., Michael, S., Pragani, R., Boxer, M., Sumita, K., Takeuchi, K., Auld, D. S., Li, Z., Cantley, L. C. and Simeonov, A. (2013) A homogeneous, high-throughput assay for phosphatidylinositol 5-phosphate 4-kinase with a novel, rapid substrate preparation. *PLoS One.* **8**, e54127
- 16 Voss, M. D., Czechtizky, W., Li, Z., Rudolph, C., Petry, S., Brummerhop, H., Langer, T., Schiffer, A. and Schaefer, H. L. (2014) Discovery and pharmacological characterization of a novel small molecule inhibitor of phosphatidylinositol-5-phosphate 4-kinase, type II, beta. *Biochem Biophys Res Commun.* **449**, 327-331
- 17 Berndt, A., Miller, S., Williams, O., Le, D. D., Houseman, B. T., Pacold, J. I., Gorrec, F., Hon, W. C., Liu, Y., Rommel, C., Gaillard, P., Ruckle, T., Schwarz, M. K., Shokat, K. M., Shaw, J. P. and Williams, R. L. (2010) The p110 delta structure: mechanisms for selectivity and potency of new PI(3)K inhibitors. *Nat Chem Biol.* **6**, 117-124
- 18 Adrian, F. J., Ding, Q., Sim, T., Velentza, A., Sloan, C., Liu, Y., Zhang, G., Hur, W., Ding, S., Manley, P., Mestan, J., Fabbro, D. and Gray, N. S. (2006) Allosteric inhibitors of Bcr-abl-dependent cell proliferation. *Nat Chem Biol.* **2**, 95-102
- 19 Bligh, E. G. and Dyer, W. J. (1959) A rapid method of total lipid extraction and purification. *Can. J. Biochem. Physiol.* **37**, 911-917
- 20 Vadas, O., Dbouk, H. A., Shymanets, A., Perisic, O., Burke, J. E., Abi Saab, W. F., Khalil, B. D., Harteneck, C., Bresnick, A. R., Nurnberg, B., Backer, J. M. and Williams, R. L. (2013) Molecular determinants of PI3Kgamma-mediated activation downstream of G-protein-coupled receptors (GPCRs). *Proc Natl Acad Sci U S A.* **110**, 18862-18867
- 21 Burke, J. E., Perisic, O., Masson, G. R., Vadas, O. and Williams, R. L. (2012) Oncogenic mutations mimic and enhance dynamic events in the natural activation of phosphoinositide 3-kinase p110alpha (PIK3CA). *Proc Natl Acad Sci U S A.* **109**, 15259-15264
- 22 Duong Van Huyen, J., Bens, M. and Vandewalle, A. (1998) Differential effects of aldosterone and vasopressin on chloride fluxes in transimmortalized mouse cortical collecting duct cells. *J. Memb. Biol.* **164**, 79-90
- 23 Duong Van Huyen, J. P., Bens, M., Teulon, J. and Vandewalle, A. (2001) Vasopressin-stimulated chloride transport in transimmortalized mouse cell lines derived from the distal convoluted tubule and cortical and inner medullary collecting

- ducts. *Nephrology, dialysis, transplantation : official publication of the European Dialysis and Transplant Association - European Renal Association*. **16**, 238-245
- 24 Liang, Q., Dexheimer, T. S., Zhang, P., Rosenthal, A. S., Villamil, M. A., You, C., Zhang, Q., Chen, J., Ott, C. A., Sun, H., Luci, D. K., Yuan, B., Simeonov, A., Jadhav, A., Xiao, H., Wang, Y., Maloney, D. J. and Zhuang, Z. (2014) A selective USP1-UAF1 inhibitor links deubiquitination to DNA damage responses. *Nat. Chem Biol.* **10**, 298-304
- 25 Burke, J. E., Vadas, O., Berndt, A., Finegan, T., Perisic, O. and Williams, R. L. (2011) Dynamics of the phosphoinositide 3-kinase p110delta interaction with p85alpha and membranes reveals aspects of regulation distinct from p110alpha. *Structure* **19**, 1127-1137
- 26 Kunz, J., Wilson, M. P., Kisseleva, M., Hurley, J. H., Majerus, P. W. and Anderson, R. A. (2000) The activation loop of phosphatidylinositol phosphate kinases determines signaling specificity. *Mol Cell*. **5**, 1-11.
- 27 Kunz, J., Fuelling, A., Kolbe, L. and Anderson, R. A. (2002) Stereo-specific substrate recognition by phosphatidylinositol phosphate kinases is swapped by changing a single amino acid residue. *J Biol Chem*. **277**, 5611-5619.
- 28 Thorsell, A. G. and al, e. (2006) PIP5KC2: Human phosphatidylinositol-4-phosphate 5-kinase , type II, gamma. RCSB PDB. DOI:10.2210/pdb2gk9/pdb
- 29 Rao, V. D., Misra, S., Boronenkov, I. V., Anderson, R. A. and Hurley, J. H. (1998) Structure of type IIbeta phosphatidylinositol phosphate kinase: a protein kinase fold flattened for interfacial phosphorylation. *Cell*. **94**, 829-839
- 30 Gonin, S., Deschenes, G., Roger, F., Bens, M., Martin, P. Y., Carpentier, J. L., Vandewalle, A., Doucet, A. and Feraille, E. (2001) Cyclic AMP increases cell surface expression of functional Na,K-ATPase units in mammalian cortical collecting duct principal cells. *Mol Biol Cell*. **12**, 255-264
- 31 Maeda, A., Amano, M., Fukata, Y. and Kaibuchi, K. (2002) Translocation of Na(+),K(+)-ATPase is induced by Rho small GTPase in renal epithelial cells. *Biochem Biophys Res Commun*. **297**, 1231-1237
- 32 Ngok, S. P., Lin, W. H. and Anastasiadis, P. Z. (2014) Establishment of epithelial polarity - GEF who's minding the GAP? *J Cell Sci*. **127**, 3205-3215

Figure Legends

Figure 1 Structure of NIH-12848

Figure 2 Effect of inhibitor NIH-12848 on PI5P4K γ activity.

A) Dose-response curve showing inhibition of PI5P 4-kinase activity over a range of inhibitor concentrations (0.01 to 100 μ M). Points represent a mean of 5 replicates and error bars indicate \pm S.E.M. B) Effect of a range of inhibitor concentrations on intrinsic ATPase activity of PI5P4K γ . Bars represent % ATP conversion by PI5P4K γ (1 μ M) in the presence of NIH-12848, in comparison to the indicated positive control (\bullet ; 1 μ M PI5P4K γ in the absence of inhibitor). A negative control was also included (\blacksquare ; inhibitor only, no enzyme). N=3, error bars represent \pm S.E.M.

Figure 3 Binding of NIH-12848 to PI5P4K γ studied by HDX-MS.

A) Global H/D exchange of Apo PI5P4K γ . B) Structure of PI5P4K γ with changes induced by 10 μ M NIH-12848 shown in pseudo-colour. C) Summary of changes induced by NIH-12848. D) Kinetics of H/D exchange \pm 10 μ M NIH-12848 in two regions of PI5P4K γ . E) Quantification of H/D exchange in region of residues 158-162 in PI5P4K γ and PI5P4K γ + with or without NIH-12848. F) Model of PI5P4K γ active site [28] with residues mutated in this study highlighted in red (note that the E153T mutation engineered in PI5P4K γ + [12] is highlighted here in yellow – see text). The activation loop (containing Gln378) is not visible in the X-ray structure, and is a conjectural conformation, as is the location of the ATP and PI5P substrates. Also in yellow (but not indicated) are Asp374, which is a conserved aspartate crucial for ATP binding [29], and Ala386, which dictates the substrate specificity of PI5P4Ks [26, 27].

Figure 4 Effect of inhibitor NIH-12848 on PI5P4K γ harbouring a single amino acid substitution.

PI5P4K γ mutant N165I was assayed in the presence of 0, 5 and 50 μ M NIH-12848 and showed no significant sensitivity towards this inhibitor. N= 3-6 replicates for each condition, error bars represent S.E.M.

Figure 5 Effects of NIH-12848 on mpkCCD cells.

A) Effect of 10 μ M NIH-12848 on Na⁺/K⁺ ATPase α -1 localization. Cells were grown on glass coverslips at sub-confluence and then treated for 24 h with inhibitor or carrier (DMSO). They were stained for ZO-1 (gap junctions) or Na⁺/K⁺ ATPase α -1 and viewed under a confocal microscope. Low resolution imaging showed that >90% of the cells were as shown in these higher resolution images, and at least three experiments were performed with identical results. Objective 100X. Bars, 10 μ m.

B) Effect of 10 μ M NIH-12848 on dome formation. Cells were grown on plastic dishes to confluence (no domes present) and then for a further 48 hours with inhibitor or carrier. Phase contrast images of cell monolayers are shown. Objective 20X. Bars, 50 μ m.

C) Effect of 10 μ M NIH-12848 after domes have formed. Cells were grown on plastic dishes for 5 days to allow dome formation and then with inhibitor or carrier for a further 24 hours. Phase contrast images of cell monolayers are shown. Objective 20X. Bars, 50 μ m.

Figure 6

A) Specificity and depletion efficiency of PI5P4K γ siRNA. mpkCCD cells grown on plastic dishes were transfected with control siRNA or PI5P4K γ -specific siRNA. After 72 hours, the transfection was repeated. After further 48 hours, RNA was extracted and the expression levels of each PI5P4K isoform was evaluated by RT-qPCR. Values (above) are expressed as fold difference in knocked-down cells relative to control cells with TATA-box binding protein (TBP) as the reference gene. Depletion of PI5P4K γ was also evaluated in cell lysates by Western blot (below). Equal volumes of cell lysates were loaded on a 10% SDS-PAGE gel and PI5P4K γ was detected with an isoform-specific polyclonal antibody (see Methods).

B) Effect of siRNA knock-down of PI5P4K γ on Na⁺/K⁺-ATPase α -1 localization. Cells grown on glass coverslips were depleted of endogenous PI5P4K γ by siRNA as described in Material and Methods. Confocal sections of cells fixed and stained for Na⁺/K⁺-ATPase α -1 (green) and ZO-1 (red) are shown. These images are typical of two independent experiments, and the images are representative of >90% of cells examined. Objective 63X. Bars, 10 μ m.

C) Effect of siRNA knock down of PI5P4K γ on dome formation. mpkCCD cells grown on plastic dishes were depleted of endogenous PI5P4K γ by siRNA as described in Material and Methods. Phase contrast images of cell monolayers are shown. Objective 10X. Bars, 50 μ m.

D) Surface density of cell domes was measured in mpkCCD confluent cell monolayers that were transfected with PI5P4K γ -specific siRNA or only transfection reagent (Control 2) or Non Target Oligos siRNA (Control 3). In Control 1 cells were not transfected. Values are expressed as means \pm SEM. * p <0.001 versus Control 3. Significant differences were analyzed by Student's t -test.

.Table 1

mRNA levels of PI5P4Ks in mpkCCD cells grown to confluence

Gene	PI5P4Kγ	PI5P4Kα	PI5P4Kβ
Polarized mpkCCD cells	3.19-3.46	0.99-1.01	0.51-0.53

The relative expression of the three genes PI5P4K γ , α , and β , with TATA-box binding protein as a reference gene, was determined in a RT-qPCR assay. Values are expressed as fold difference in polarized cells (four days after reaching confluence when domes are formed) relative to pre-confluent cells (no domes present).

Figure 1

NIH-12848

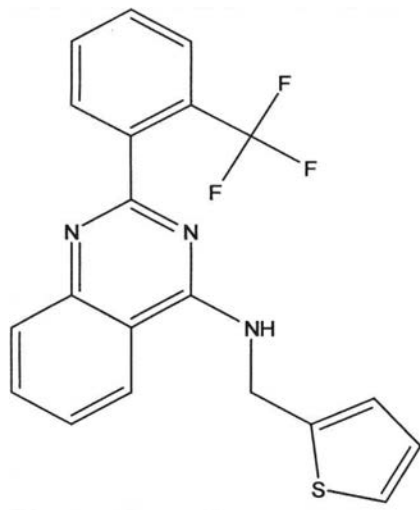


Figure 2

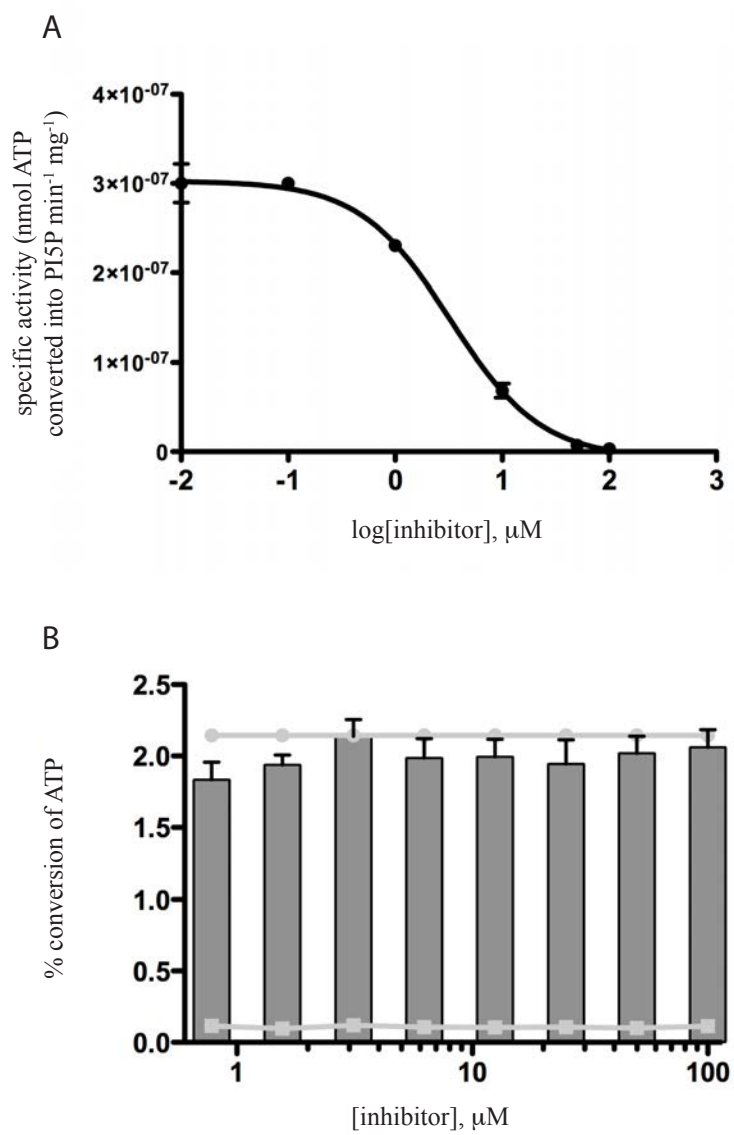


Figure 3

HDX-MS

Fig 3A

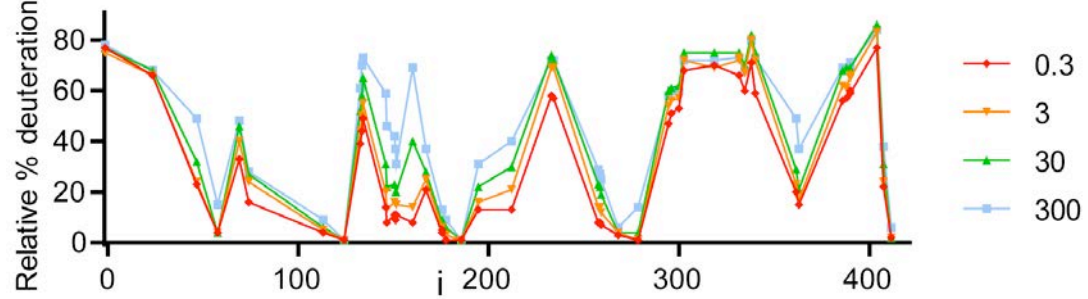


Fig 3B

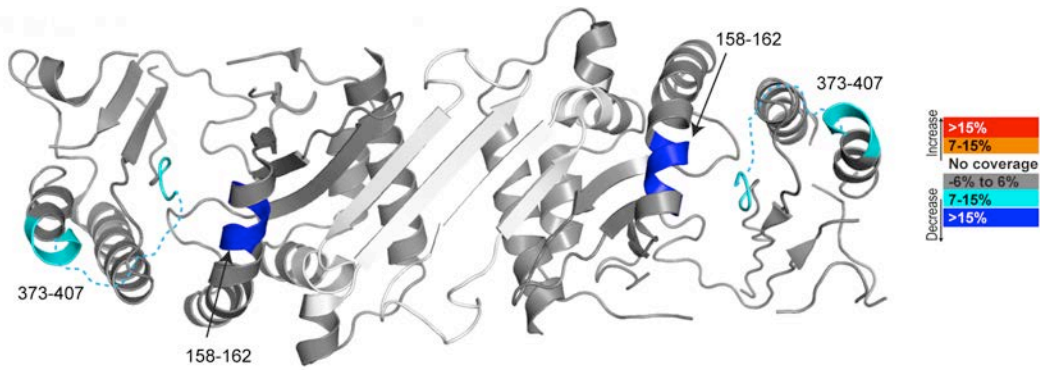


Fig 3C

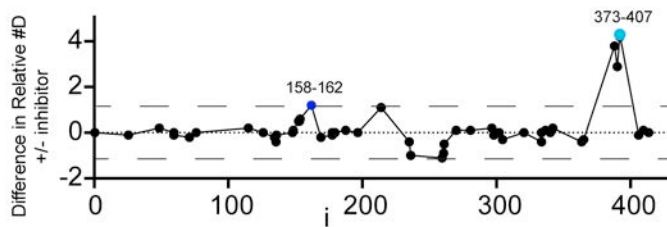


Fig 3D

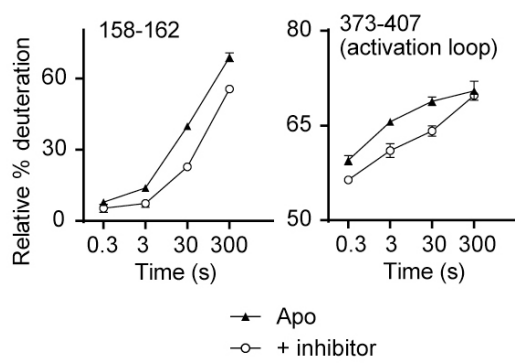


Fig 3E

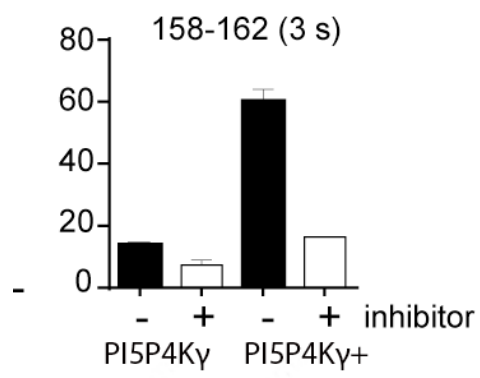


Fig 3F

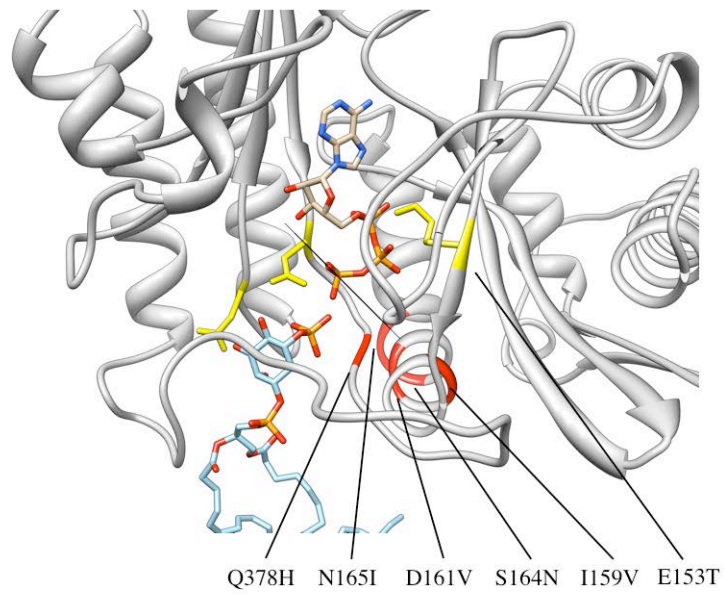


Figure 4

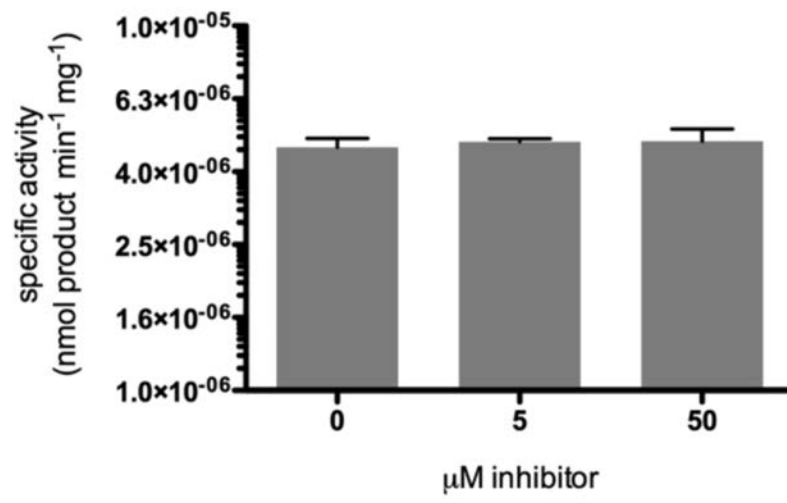


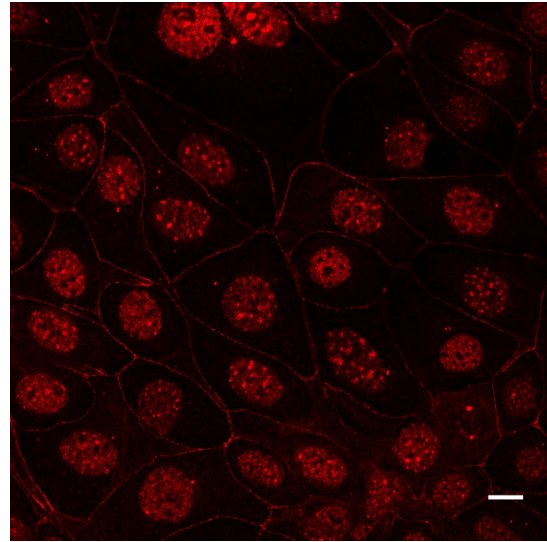
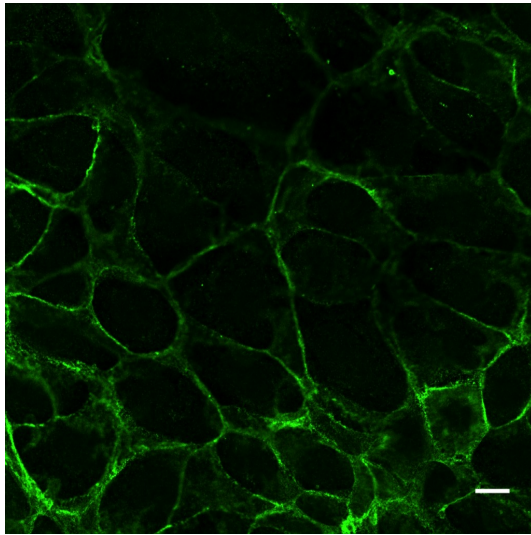
Figure 5

Fig 5A

Na⁺/K⁺ ATPase α -1

ZO-1

Control



+ NIH-12848

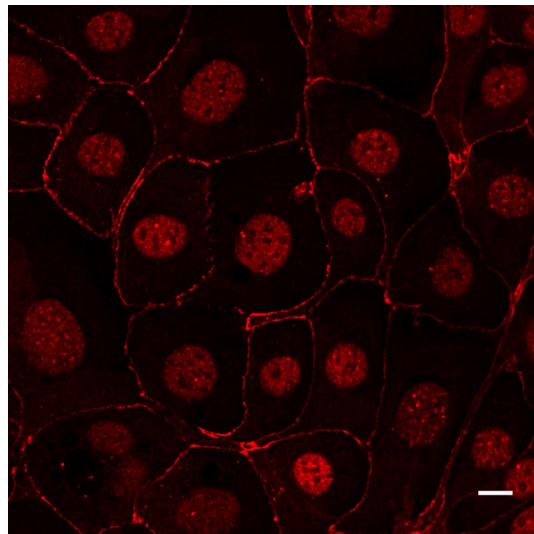
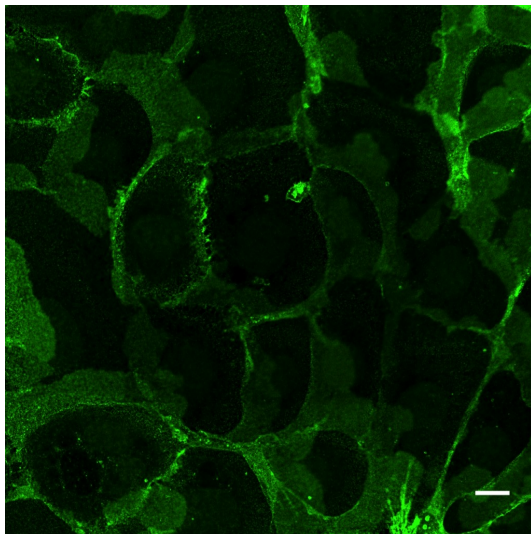
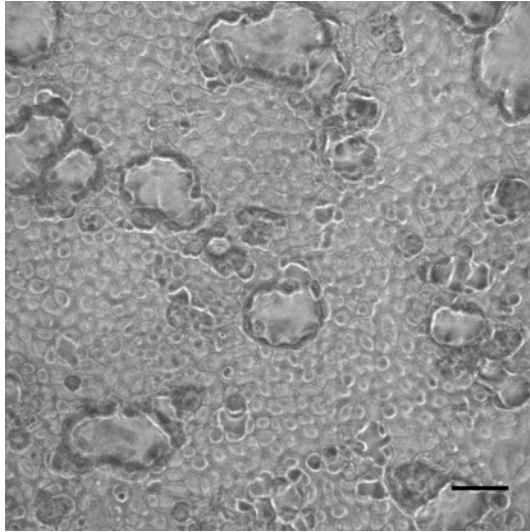


Fig 5B

Control



+ NIH-12848

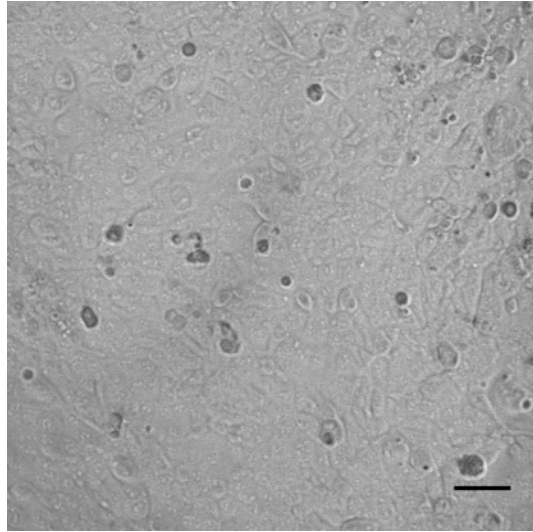
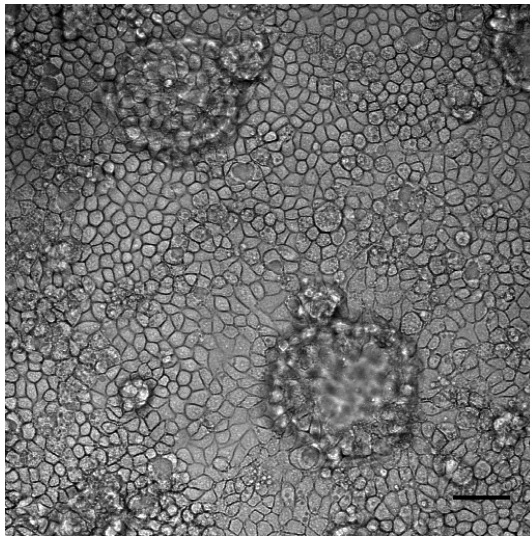


Fig 5C

Control



+ NIH-12848

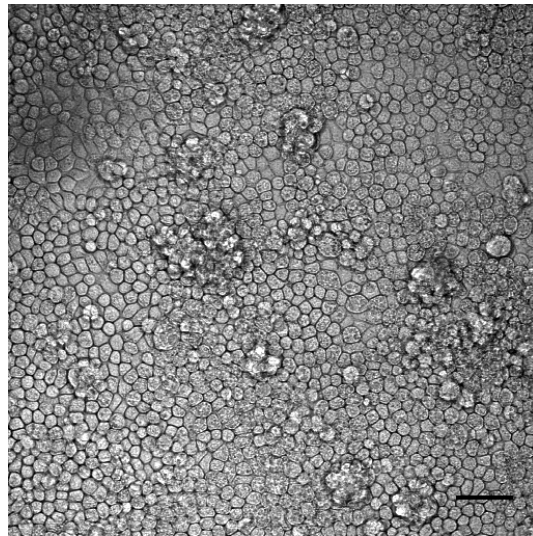


Figure 6

Fig 6A

Gene	PI5P4Kγ	PI5P4Kα	PI5P4Kβ
Relative mRNA expression	0.16-0.18	0.92-0.98	0.81-0.84

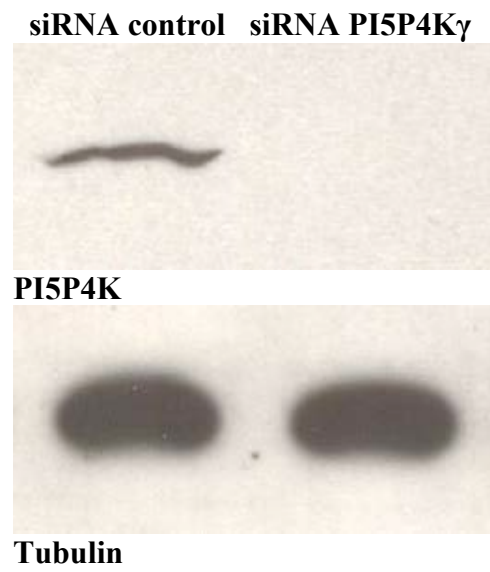
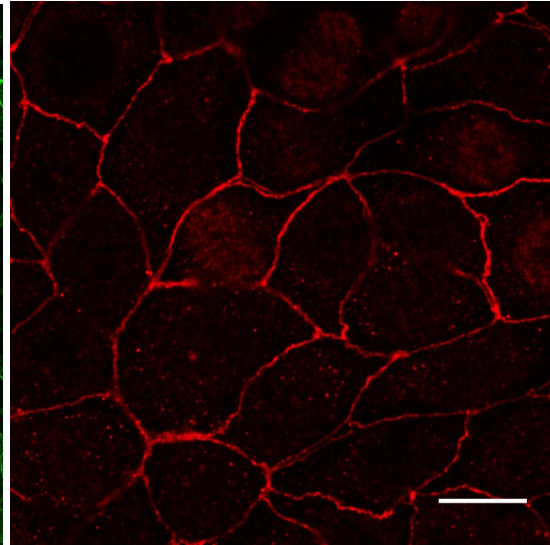
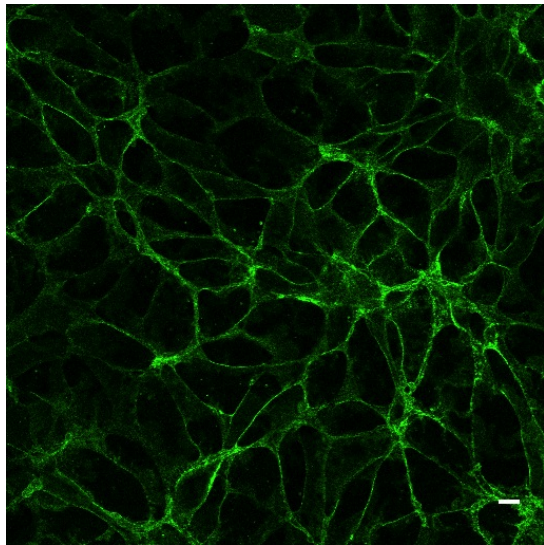


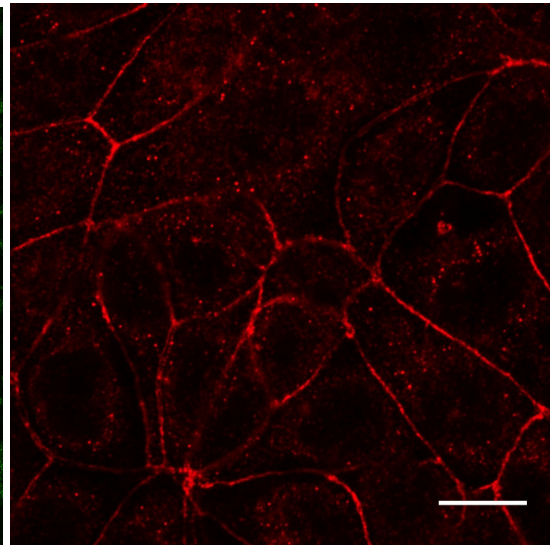
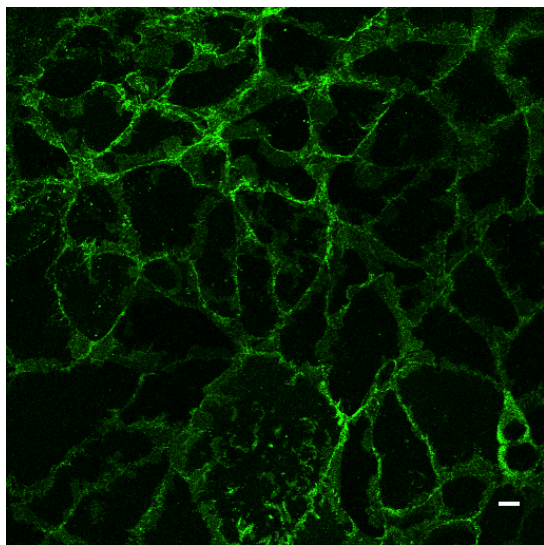
Fig 6B

Na⁺/K⁺-ATPase α -1

ZO-1



siRNA control



siRNA-PI5P4K γ

Fig 6C

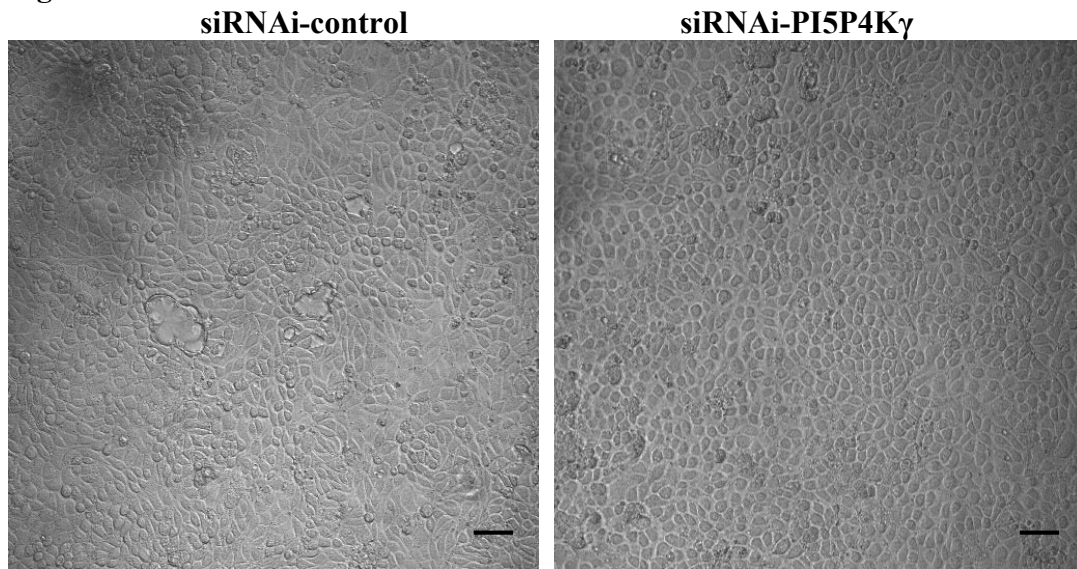
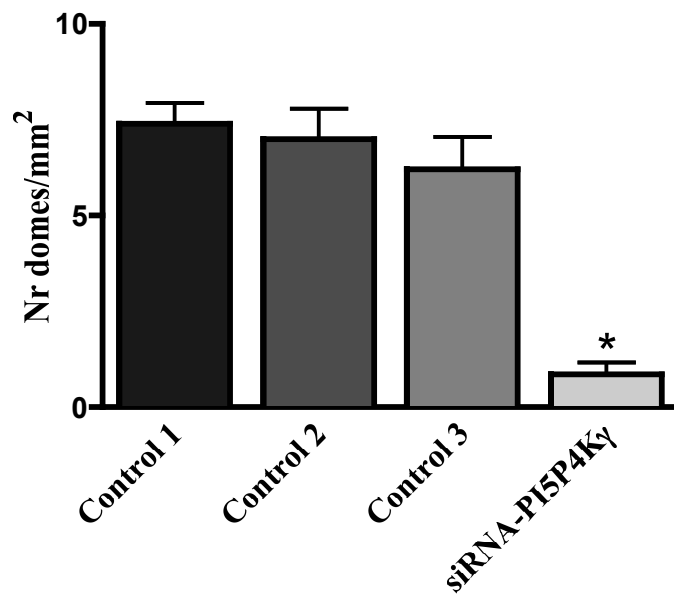


Fig 6D



Supplementary Tables

Supplementary Table 1.

Primer pairs that were used to generate amino acid substitutions in PI5P4K γ and PI5P4K γ + mutants.

Amino acid change	Primer pair (forward/reverse)
Q378H	5'-TATCCTTACACATTATGATGCCAAGAAG 5'-TGGCATCATAATGTGTAAAGGATATCAATG
I159V + D161E	5'-CCAGTGAGGACGTTGCTGAAATGCATAGCAAC 5'-GCTATGCATTTTCAGCAACGTCCTCACTGGATACTG
S164N	5'-TGACATGCATAACAACCTCTCCAACATCAC 5'-AGTTGGAGAGGTTGTTATGCATGTCAGCAATG
N165I	5'-TGACATGCATAGCATCCTCTCCAACATCAC 5'-AGTTGGAGAGGATGCTATGCATGTCAGCAATG

Supplementary Table 2

Data from Kinome screen (see xls file)

Supplementary Table 3

mRNA levels of PI5P4Ks following RNAi induced knock down.

Relative mRNA expression	PI5P4K γ	PI5P4K α	PI5P4K β
si-RNA-PI5P4K γ	0.16-0.18	0.92-0.98	0.81-0.84
siRNA-PI5P4K α	1.10-1.40	0.15-0.20	1.00-1.10
siRNA-PI5P4K β	1.00-1.20	0.84-0.98	0.30-0.32

mpkCCD cells grown on plastic dishes were transfected with control siRNA or PI5P4K-specific siRNAs. After 72 hours, transfection was repeated. After further 48 hours, RNA was extracted and the expression levels of each PI5P4K isoform was evaluated by RT-qPCR.

Supplementary Figures

Supplementary Figure Legends

Figure S1

Dose-response of NIH-12848 on PI5P4K γ in Kinome screen.

Figure S2

Data for PIP kinases extracted from Supplementary Table S2

Figure S3

Effect of inhibitor NIH-12848 on PI5P4K activity. Specific activities of PI5P4K α (A) and PI5P4K β (B) are not inhibited when assayed in the presence of NIH-12848. N=3, error bars represent \pm S.E.M. C) Dose response curve of PI5P4K γ + inhibited by NIH-12848. Values represent mean reduced activity compared to the mean of uninhibited PI5P4K γ + replicates from the same experiment.

Figure S4

Effect of inhibitor NIH-12848 on the activity of PI5P4K γ mutants. A) Specific activity of PI5P4K γ and B) PI5P4K γ +, both with five amino acid substitutions (Q378H, I159V, D161E, S164N and N165I) were assayed in the presence of 0, 5 and 50 μ M NIH-12848 inhibitor. C) Specific activity of PI5P4K γ with a single amino acid substitution (S164N) in the presence of 1, 2 and 5 μ M NIH-12848 inhibitor. D) Summary of the specific activities of a full range of PI5P4K γ mutants in the presence of no (-) or 5 μ M (+) NIH-12848. Substituted amino acids are listed below the relevant bars. WT = wild type PI5P4K γ . N= a minimum of 3 replicates for each experiment, error bars represent S.E.M.

Figure S5

Effects of RNAi knockdown of PI5P4K α and β on dome formation in mpkCCD cells. A) siRNA for PI5P4K α or control were applied in two rounds over 5 days. Typical images are shown. B) Quantification of experiments typified by Fig S5A (with data for equivalent experiments with siRNA for PI5P4K β) Values are expressed as means \pm SEM. * p <0.001. Significant differences were analyzed by Student's *t*-test. C) Quantification of experiments in which PI5P4K α and γ were knocked down alone or together. Values are expressed as means \pm SEM. * p <0.001. Significant differences were analyzed by Student's *t*-test.

Supplementary Figures

Figure S1

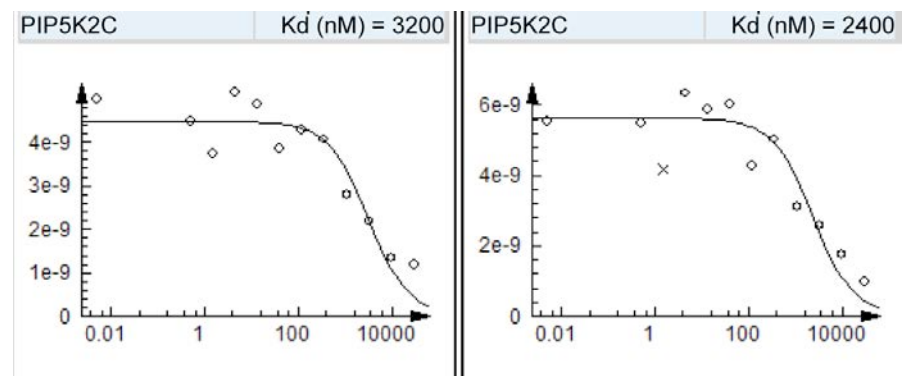


Figure S2

PIP5K1A	100
PIP5K1C	100
PIP5K2B	100
PIP5K2C	8.8

Figure S3

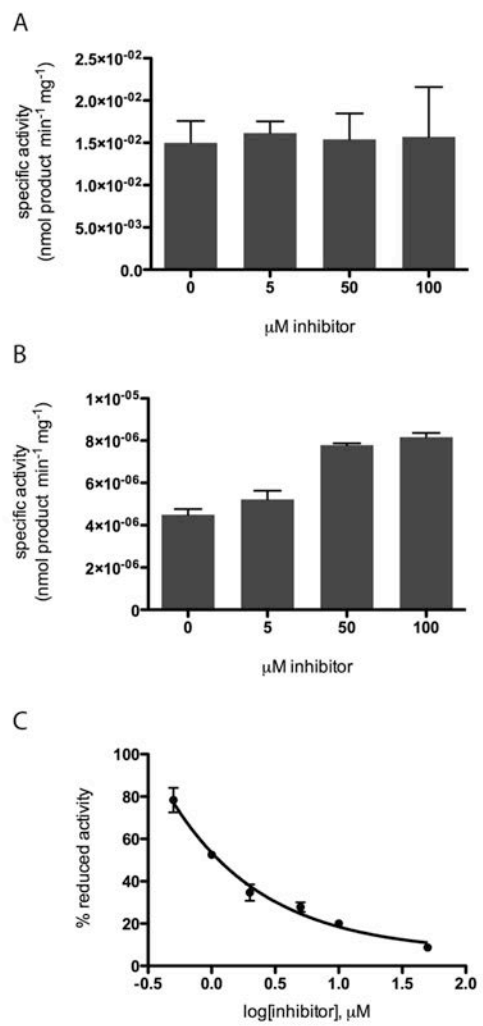


Figure S4

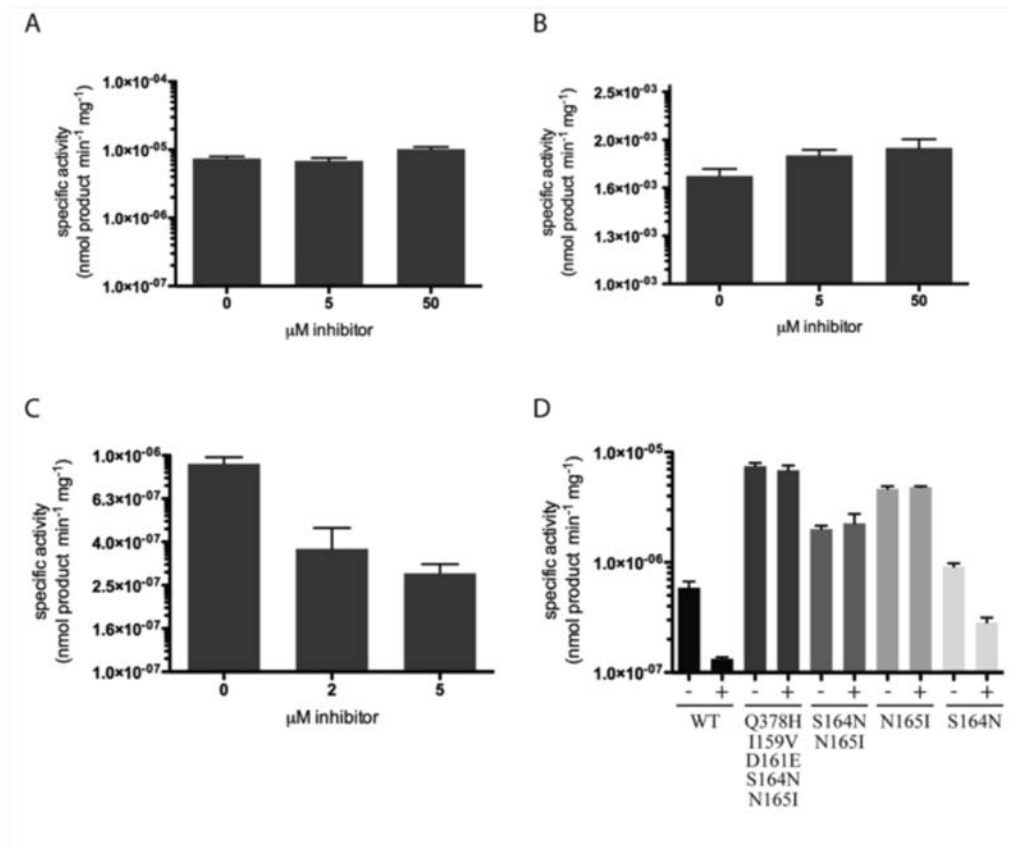
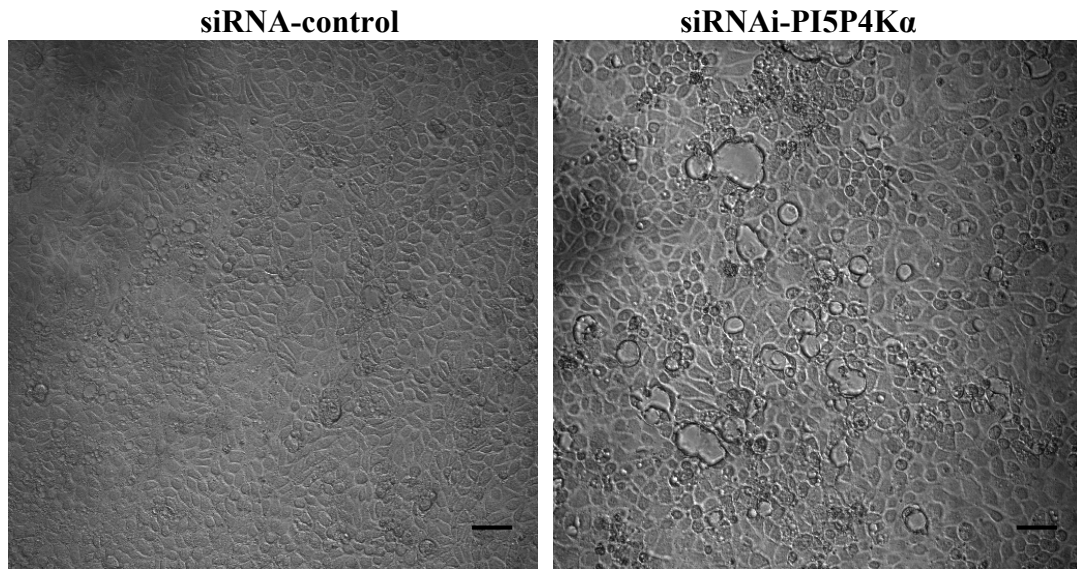


Figure S5

S5A



S5B

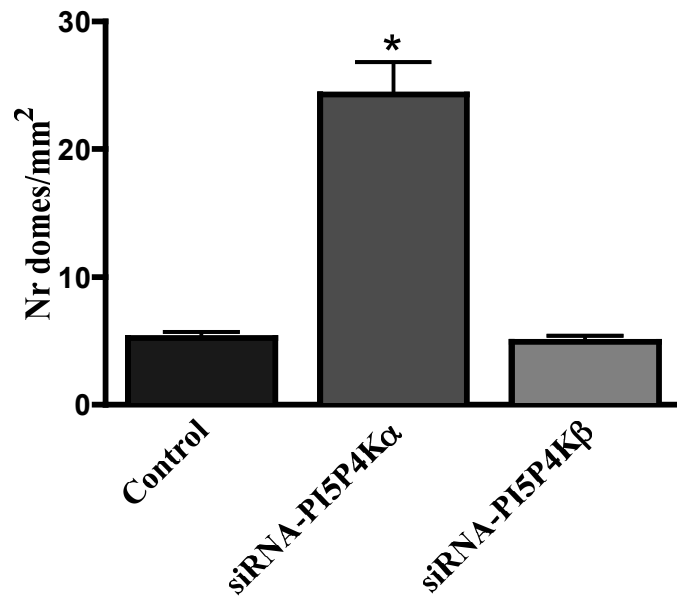


Fig S5C

